Hardware Efficient Quantum Simulation of Non-Abelian Gauge Theories with Qudits on Rydberg Platforms

Daniel González-Cuadra,[1,2,*,†] Torsten V. Zache,[1,2,*,‡] Jose Carrasco,[1] Barbara Kraus,[1] and Peter Zoller[1,2]
[1]Institute for Theoretical Physics, University of Innsbruck, 6020 Innsbruck, Austria
[2]Institute for Quantum Optics and Quantum Information of the Austrian Academy of Sciences, 6020 Innsbruck, Austria

(Received 29 March 2022; revised 12 July 2022; accepted 27 September 2022; published 13 October 2022)

Non-Abelian gauge theories underlie our understanding of fundamental forces in nature, and developing tailored quantum hardware and algorithms to simulate them is an outstanding challenge in the rapidly evolving field of quantum simulation. Here we take an approach where gauge fields, discretized in spacetime, are represented by qudits and are time evolved in Trotter steps with multiqudit quantum gates. This maps naturally and hardware efficiently to an architecture based on Rydberg tweezer arrays, where long-lived internal atomic states represent qudits, and the required quantum gates are performed as holonomic operations supported by a Rydberg blockade mechanism. We illustrate our proposal for a minimal digitization of SU(2) gauge fields, demonstrating a significant reduction in circuit depth and gate errors in comparison to a traditional qubit-based approach, which puts simulations of non-Abelian gauge theories within reach of NISQ devices.

DOI: 10.1103/PhysRevLett.129.160501

Introduction.—Quantum field theories form the backbone of the standard model of particle physics, where quantized gauge fields mediate the interactions between fundamental particles [1]. Lattice gauge theories (LGTs), where fields are discretized on a space-time lattice [2], provide a convenient framework to study nonperturbative high-energy phenomena, and have been extensively used to extract numerous experimentally relevant predictions [3]. Despite this success, standard approaches based on Monte Carlo methods are severely limited by the sign problem [4], preventing the study of real-time gauge theory dynamics, among other drawbacks. The latter are essential to analyze experimental results in heavy-ion colliders, where open problems in particle physics are currently being addressed [5,6], including the search of new physics beyond the standard model.

In the recent years, quantum simulators (QS) [7] have emerged as a promising pathway to circumvent these problems [8–13], leading to several experimental demonstrations where simple LGTs were investigated using digital, analog, and variational methods [14–20]. For digital QS [21], in particular, different schemes have been proposed to address high-dimensional non-Abelian gauge theories using different platforms, including trapped ions [22–24], ultracold atoms [25–29], superconducting circuits [30–32], and cavities [33]. Despite their higher flexibility to simulate complex many-body Hamiltonians compared to the analog approach, crucial in particular for non-Abelian theories, a full digital quantum simulation requires access to gate-based quantum computers, which are currently restricted to noisy intermediate scale quantum (NISQ) devices [34], limited in qubit number and circuit depths. Although an impressive effort is currently taking place to reduce the computational complexity using improved quantum software [35–49], simulating relevant LGTs in the NISQ era must be complemented by the development of efficient quantum hardware tailored to the specific algorithmic demands.

In this Letter, we introduce a qudit architecture based on atoms trapped in optical tweezer arrays and laser excited to Rydberg states [50–56] (Fig. 1). We co-design the platform to match the requirements to digitally simulate real-time dynamics of non-Abelian gauge theories in a hardware-efficient manner. In particular, we show a considerable reduction of experimental resources compared to qubit-based approaches due to a more natural match between the simulating and the simulated degrees of freedom, preserving the local structure of gauge-invariant interactions.

Although qudit-based quantum simulators can also be implemented with other platforms such as ultracold mixtures [57], trapped ions [58] and photonic circuits [59], multidimensional tweezer arrays, both dynamically reconfigurable and locally addressable [53,56,60–63], satisfy the scalability requirements necessary to address the continuum limit of LGTs. Specifically, here we consider multilevel atoms to encode large gauge-field Hilbert spaces using long-lived qudits [64–66]. Employing a Rydberg blockade mechanism [51,52,67], we develop a native set of holonomic gates [68–72], robust against decoherence, that allows to efficiently simulate the time evolution under a general LGT Hamiltonian. In particular, we show how for the simplest nontrivial digitization of SU(2) gauge fields, and including relevant error sources, our qudit approach achieves higher fidelities than a traditional qubit protocol

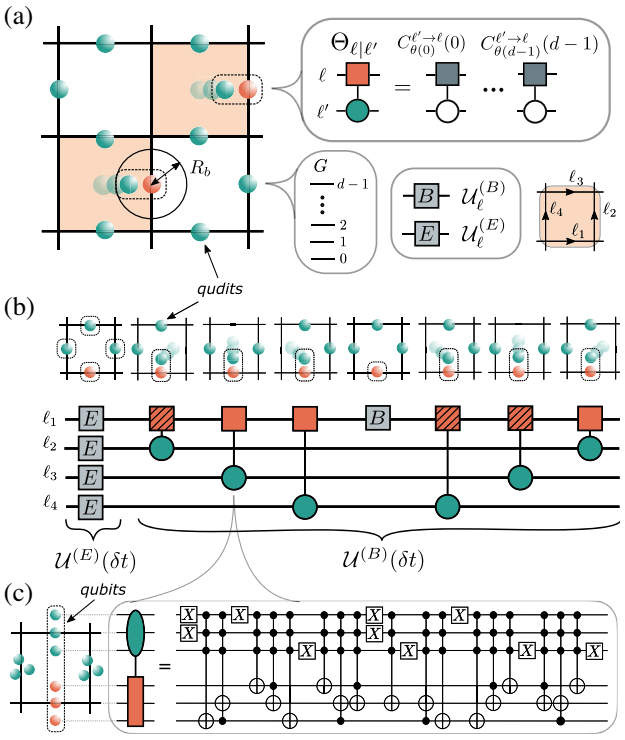

FIG. 1. Gauge field dynamics on qudit vs qubit quantum simulator: (a) Our proposal employs Rydberg atoms trapped in optical tweezers, arranged on the links ℓ of a hypercubic lattice. Each atom encodes a qudit using d internal levels, where single-qudit gates are realized holonomically. To implement the entangling two-qudit gate $\Theta_{\ell|\ell'}$ we first bring pairs of atoms within the Rydberg blockade radius R_b. (b) First order decomposition of a Trotter step, including the four-qudit plaquette interaction, into the native atomic gates $\mathcal{U}^{(E/B)}_\ell$ and $\Theta_{\ell|\ell'}$. (c) For comparison, we show a qubit-based circuit decomposition of $\Theta_{\ell|\ell'}$ for the Q_8 group, where the number of required atoms is increased by a factor $\log_2 8 = 3$, leading to much lower gate fidelities, while our qudit approach enables a faithful simulation [see Figs. 2(c) and 2(d)].

[73], enabling the quantum simulation of non-Abelian gauge theories using NISQ devices [53]. Finally, we note that although larger qudit sizes are required to properly approximate the physics of SU(2) as relevant for high-energy physics [37], this minimal protocol can readily be employed to study condensed matter systems with non-Abelian topological order [75,76].

Qudit quantum computing with Rydberg atoms.—Atomic systems offer the possibility to encode quantum information in internal states. Here, we go beyond the paradigmatic model of a two-level atomic qubit and consider a collection of N multilevel atoms in state-independent optical traps. For every single atom, we propose to encode a *qudit* with corresponding Hilbert space spanned by $|j\rangle$, $j = 0, \ldots, d-1$ in d long-lived hyperfine ground states $|F, m_F\rangle$, where large hyperfine manifolds can be accessed, e.g., using erbium [77] or holmium [78,79]. In a qubit-based approach, an equivalent Hilbert space of dimension d^N requires control over $N\log_2(d)$ instead of only N atoms as in our case [Fig. 1(c)]. This saving of physical resources is crucial for efficient near-future applications in the NISQ era, since the number of atoms that can be trapped and controlled is limited. For instance, a 4×4 2D lattice containing 32 $d = 8$ qudits (which will become relevant later) could be encoded using 32 atoms, a number that is already available [53], while almost 100 of them should be used instead in a qubit-based protocol.

The quantum information stored in each atomic qudit can be efficiently manipulated, e.g., using holonomic operations [68,80], where arbitrary single-qudit gates $U \in \mathrm{SU}(d)$ can be synthesized via an appropriate sequence of laser pulses, with time-dependent Rabi frequencies $\Omega(t)$. To see this, we first decompose U into a product of at most $d(d-1)/2$ unitaries acting nontrivially only on two atomic levels (i, j) [81], and subsequently realize the two-level unitaries via at most three rotations around the x or y axis, denoted by $R^{(i,j)}_{x(y)}(\varphi)$, respectively, utilizing an auxiliary state $|e\rangle$ (see the Supplemental Material [82] for details). The total time required to implement a general single-qudit gate is upper bounded by $3d(d-1)T/2$, where T is the duration of a laser pulse, estimated below for realistic experimental parameters. We note that the explicit implementation of this scheme should be guided by the constraints imposed by atomic selection rules, see Fig. 2(a) for an example with $d = 8$.

The main error sources affecting the fidelity of single-qudit gates are the spontaneous decay from the excited state $|e\rangle$ [Fig. 2(a)] as well as nonadiabatic state transfer. As we show in Ref. [82], both can be made negligible by imposing $\Omega \gg 1/T$, γ_e, which can be achieved in current experiments. The fast and high fidelity single-qudit gates obtained with our protocol [82] contrast with those achievable in a qubit-based approach, where $\mathcal{O}(d^2)$ entangling CNOT gates between $\log d$ qubits are required, leading to larger errors and longer implementation times.

We now come to the main challenge of qudit quantum computing and introduce a new protocol for a general class of controlled-unitary operation, $C_U(j_0) = U \otimes |j_0\rangle\langle j_0| + \mathbb{1} \otimes (\mathbb{1} - |j_0\rangle\langle j_0|)$ with $j_0 \in \{0, \ldots d-1\}$. Our proposal is based on the Rydberg blockade mechanism [51,52,67], which prohibits the simultaneous excitation of two atoms to the Rydberg state $|r\rangle$ when their distance R is below the blockade radius, R_b, set by the large Rydberg interaction $V \sim 1/R^6 \gg \Omega$. This idea gives rise to the following protocol. First, bring the control and target atoms within range $R < R_\mathrm{b}$ and apply the unitary U on target (as outlined above). Now excite the control qudit from $|j_0\rangle$ to the Rydberg state $|r\rangle$ using $S_{(j_0,r)} \equiv R^{(j_0,r)}_y(\pi)$, and subsequently realize $U^\dagger$ on the target by decomposing every two-level rotation as $R^{(i,j)}_{x/y}(\varphi) = S^\dagger_{(i,r)} R^{(j,r)}_{x/y}(\varphi) S_{(i,r)}$ [Fig. 2(b)].

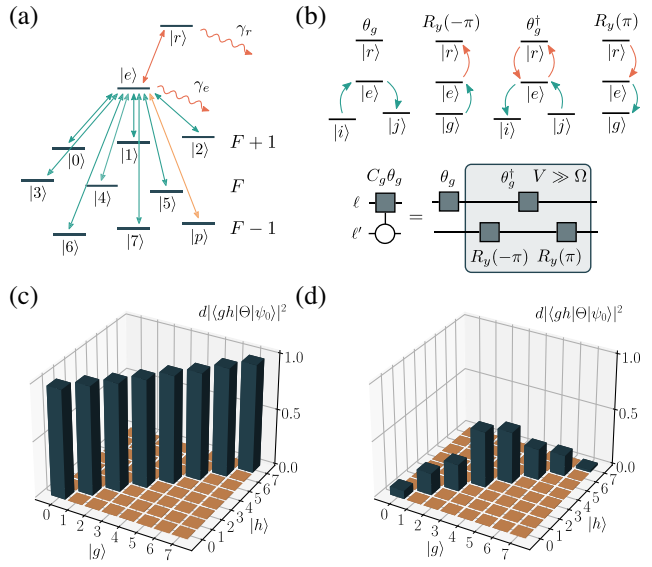

FIG. 2. Qudit encoding and native gates: (a) Atomic level structure serving as a Q_8 register, where the $d = 8$ group basis elements are encoded into different hyperfine manifolds. Single and two-qudit gates are performed holonomically using the auxiliary ground-state level $|p\rangle$ and excited states $|e\rangle$ and $|r\rangle$, with corresponding decay rates $\gamma_{e/r}$. (b) Controlled-permutation gate $C^{\ell'\to\ell}_{\theta(g)}(g)$ as a sequence of four single qudit gates in the blockade regime. Quantified by the maximally entangled state obtained after applying $\Theta_{\ell|\ell'}$ to $|\Psi_0\rangle$, implemented through the (c) qudit and (d) qubit protocols [see the circuit in Fig. 1(c)] using the same experimental parameters (see main text), we obtain a state fidelity of 99.6% and 21.4%, respectively, demonstrating the clear advantage of a qudit-based decomposition.

To emphasize the involvement of the Rydberg state we denote this gate by $U_r^\dagger$. Finally, applying $S^\dagger_{j_0,r}$ to the control qudit maps the state $|r\rangle$ back to $|j_0\rangle$. Because of the Rydberg blockade, which projects onto the subspace orthogonal to the state $|rr\rangle$ (both atoms in the Rydberg state), this protocol realizes the operator

$$(\mathbb{1}\otimes S^\dagger_{(j_0,r)})[\mathcal{P}(U_r^\dagger\otimes\mathbb{1})\mathcal{P}](\mathbb{1}\otimes S_{(j_0,r)})(U\otimes\mathbb{1}), \quad (1)$$

with $\mathcal{P} = \mathbb{1} - |rr\rangle\langle rr|$. If this operator acts on states where the Rydberg states are not populated, it coincides with $C_U(j_0)$. That is, U is applied to the target qudit *if and only if* the control qudit was in state $|j_0\rangle$. The execution time of this gate is upper bounded by $[6d(d-1)+2]T$. Apart from the error sources mentioned above, imperfect Rydberg blockade and decay from the Rydberg state can lower the fidelity of controlled-unitary gates. Below we discuss how the latter affect the simulation of non-Abelian LGTs for a minimal example with $d = 8$.

In summary, we have established a gate set $\mathcal{G} = \{U, C_U(j_0)\}$ consisting of arbitrary single-qudit gates $U \in SU(d)$ and controlled two-qudit gates $C_U(j_0) \in SU(d^2)$. These are naturally available in a qudit register consisting of multilevel Rydberg atoms in a programmable tweezer array. The universal properties of $\mathcal{G}$ for general qudit-based algorithms will be discussed elsewhere [83]; here we are specifically interested in the simulation of LGTs as discussed in the following section.

Gauge field dynamics on a qudit quantum computer.—In this section, we turn our attention to the digital simulation of real-time gauge theory dynamics with qudits. Most importantly, we will show that the architecture outlined above provides exactly those resources which are required to simulate LGTs on a quantum device. To see this, we take the Hamiltonian lattice approach [84]. Given a gauge group G and a hypercubic lattice with N_ℓ links ℓ, we represent the state $|\psi(t)\rangle$ at time t on a so-called G register [36], $|\psi(t)\rangle = \sum_{\boldsymbol{g}} \psi_t(\boldsymbol{g})|\boldsymbol{g}\rangle$, with $|\boldsymbol{g}\rangle = |g_1\rangle_1 \otimes |g_2\rangle_2 \otimes \ldots = \otimes_\ell |g_\ell\rangle_\ell$. Here, every $|g\rangle$ denotes a state labeled by a group element $g \in G$, and the set $\{|g\rangle\}$ forms an orthonormal basis of the local (link) Hilbert space $\mathcal{H}_G$. For the relevant cases of $G = \mathrm{U}(1)$ or $\mathrm{SU}(N)$, where $\mathcal{H}_G$ is infinite dimensional, we replace G with a large, but finite subgroup of itself, which leads to $\mathcal{H}_G \simeq \mathbb{C}^{|G|}$, with dimension given by the order of the group $|G|$, and thus effectively digitizes the many-body wave function $\psi_t(\boldsymbol{g})$ [37]. The state $|\psi(t)\rangle$ can then be encoded naturally in a set of N_ℓ *qudits* by identifying the computational basis $\{|j\rangle\}$ $(j = 0, \ldots, d-1)$ with the group state basis $\{|g\rangle\}$ $(g \in G)$, with $|G| = d$ [Fig. 1(a)].

The main target of this Letter is the time-evolution operator $\mathcal{U}_G(t) = e^{-iH_G t}$ acting on a given initial state $|\psi(0)\rangle$, i.e., we aim to realize the evolution $|\psi(t)\rangle = \mathcal{U}(t)|\psi(0)\rangle$ in a *hardware-efficient* way. For a general Kogut-Susskind-type LGT, this evolution is generated by a Hamiltonian $H_G = \lambda_E H_E + \lambda_B H_B$ with "electric" (E) and "magnetic" contributions (B) [84],

$$H_E = \frac{1}{2}\sum_\ell E_\ell^2, \qquad H_B = \sum_\square (\mathcal{U}_\square + \mathcal{U}_\square^\dagger). \quad (2)$$

While the operator E_ℓ^2 acts nontrivially only on a single link ℓ, the plaquette operator

$$\mathcal{U}_\square = \mathrm{tr}[U_{\ell_1} U_{\ell_2} U^\dagger_{\ell_3} U^\dagger_{\ell_4}] \quad (3)$$

involves the four links ℓ_i with $i = 1, \ldots, 4$ of an elementary plaquette $\square$ [Fig. 1(b)]. To simplify notation we omit here and in the following the links on which $\mathcal{U}_\square$ is acting on. For $\mathrm{SU}(N)$, the U_ℓ are $N \times N$ matrices of operators [$N = 1$ for U(1)], and tr[..] denotes the corresponding trace in N dimensions [84].

We now identify the common challenges in realizing $\mathcal{U}^{(G)}(t)$ for an arbitrary (finite) group G. In our digital approach, we employ a Trotter decomposition with step size δt [85] and error of desired order $\mathcal{O}(\delta t^k)$ [86]. This reduces the task to realizing the elementary Trotter steps $\mathcal{U}^{(E/B)}(\delta t) = e^{-i\lambda_{E/B} H_{E/B}\delta t}$, as, e.g., $\mathcal{U}^{(G)}(t) = (\mathcal{U}^{(E)}(\delta t)\mathcal{U}^{(B)}(\delta t))^{t/\delta t} + \mathcal{O}(\delta t)$ for a first

order decomposition. Note that due to the locality of the interactions these steps can be applied in parallel using the local gates $\mathcal{U}_\ell^{(E)}(\delta t) = e^{-i\lambda_E E_\ell^2 \delta t}$ and $\mathcal{U}_\square^{(B)}(\delta t) = e^{-i\lambda_B(\mathcal{U}_\square + \mathcal{U}_\square^\dagger)\delta t}$. For any group G, the local gates are given by

$$\mathcal{U}_\ell^{(E)}(\delta t) = \sum_{h_\ell, g_\ell \in G} f^{(E)}(h_\ell, g_\ell, \delta t) \times |g_\ell\rangle_\ell \langle h_\ell|, \quad (4)$$

$$\mathcal{U}_\square^{(B)}(\delta t) = \sum_{g_{\ell_{1,2,3,4}} \in G} f^{(B)}(g_{\ell_1} g_{\ell_2} g_{\ell_3}^{-1} g_{\ell_4}^{-1}, \delta t) \times |g_{\ell_1}, g_{\ell_2}, g_{\ell_3}, g_{\ell_4}\rangle\langle g_{\ell_1}, g_{\ell_2}, g_{\ell_3}, g_{\ell_4}|, \quad (5)$$

acting trivially on all other links. The group dependence is encoded in the functions $f^{(E/B)}$ (see Supplemental Material [82] for explicit expressions). Hence, for $|G| = d$, $\mathcal{U}_\ell^{(E)}$ corresponds to a single-qudit gate acting on link ℓ while $\mathcal{U}_\square^{(B)}$ represents a diagonal four-qudit gate (acting on links $\ell_1, \ldots, \ell_4$).

Let us now decompose the four-qudit diagonal gate, $\mathcal{U}_\square^{(B)}$ into more elementary gates [28]. We define the two-qudit gate $\Theta_{\ell|\ell'}$, which realizes a controlled group multiplication, by $\Theta_{\ell|\ell'}|g_\ell\rangle|g_{\ell'}\rangle = |g_\ell g_{\ell'}\rangle|g_{\ell'}\rangle$. As $f^{(B)}$ depends only on the product $g_{\ell_1} g_{\ell_2} g_{\ell_3}^{-1} g_{\ell_4}^{-1} \in G$, $\mathcal{U}_\square^{(B)}$ can be implemented by applying $\Theta_{\ell|\ell'}^{(\dagger)}$ between link ℓ_1 and the other three links followed by the diagonal single-qudit gate $\mathcal{U}_\ell^{(B)}(\delta t)|g_\ell\rangle = f^{(B)}(g_\ell, \delta t)|g_\ell\rangle$, and finally undoing the first operations [Fig. 1(b)]. More explicitly,

$$\mathcal{U}_\square^{(B)} = \Theta_{\ell_1|\ell_2}^\dagger \Theta_{\ell_1|\ell_3} \Theta_{\ell_1|\ell_4} \mathcal{U}_{\ell_1}^{(B)} \Theta_{\ell_1|\ell_4}^\dagger \Theta_{\ell_1|\ell_3}^\dagger \Theta_{\ell_1|\ell_2}. \quad (6)$$

In summary, it is sufficient to realize the single-qudit gates $\mathcal{U}_\ell^{(E/B)}$ and the two-qudit gate $\Theta_{\ell|\ell'}$ for quantum simulating the real-time dynamics of an arbitrary gauge theory. The latter can be further decomposed into a product of controlled-permutation gates [Fig. 1(a)],

$$\Theta_{\ell|\ell'} = \sum_{g \in G} \theta_\ell(g) \otimes |g\rangle_{\ell'}\langle g| = \prod_{g \in G} C_{\theta(g)}^{\ell' \to \ell}(g). \quad (7)$$

Here, $\ell(\ell')$ denotes the control (target) qudit and $\theta_\ell(g)$ is a single-qudit gate implementing the right group multiplication, i.e., $\theta_\ell(g)|g_\ell\rangle = |g_\ell g\rangle$, which is just a permutation. This shows that the required gate set reduces to $\{\mathcal{U}_\ell^{(E/B)}, C_{\theta(g)}^{\ell' \to \ell}(g)\}$, which are precisely the types of gates that are naturally available with the architecture introduced in the previous section. In the spirit of codesign, we have thus identified purpose-made hardware for the digital quantum simulation of LGTs, which is the central result of this Letter. Moreover, the possibility of moving the qudits with a programmable tweezer array allows us to perform the required entangling gates in parallel (for example, at all even or odd plaquettes in two dimensions) while avoiding crosstalk from the Rydberg interaction [Fig. 1(a)], making our protocol scalable in system size.

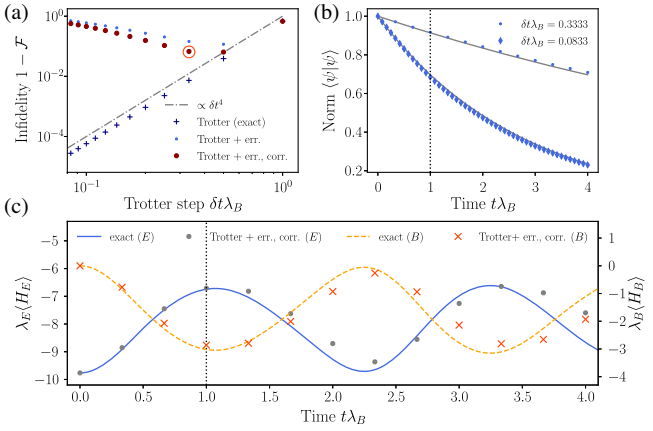

FIG. 3. Fidelity of the simulation: (a) Infidelity $1-\mathcal{F}$ of the digital simulation at final evolution time $t\lambda_B = 1$ as a function of the Trotter step $\delta t\lambda_B$, where an exact second-order Trotter decomposition (crosses) results in the scaling $1-\mathcal{F} \sim (\delta t)^4$ (dashed-dotted lines). Including gate errors, the infidelity increases again at small $\delta t\lambda_B$. Correcting for atomic losses due to decoherence, we find that optimal step size $\delta t\lambda_B = 1/3$ at the minimum of $1-\mathcal{F} \approx 6.7\%$ (red circle). (b) We measure the losses included in the simulated gates by a decay of the norm $\langle\psi|\psi\rangle$ of the time evolved state. As illustrated for the optimal and a very small Trotter step (symbols), the decay is consistent with a constant loss of ≈0.75% per Trotter step (solid lines). (c) Trotterized quench dynamics of a non-Abelian Q_8 LGT on a single plaquette for $\lambda_E/\lambda_B = 2.88$. The Trotter step corresponds to the "sweet spot" indicated in (a). Here, the observables are corrected by a multiplicative time-dependent factor due to the decay shown in (b).

Real-time dynamics of $Q_8 \subset \mathrm{SU}(2)$.—To be explicit, we now illustrate our approach for the example of the quaternion group Q_8, which is the smallest non-Abelian subgroup of SU(2) and requires qudits of size $d = 8$ [82]. Figure 3(c) shows Trotter quench dynamics in comparison to the exact result on a single plaquette, demonstrating that the expected interchange between magnetic and electric energies can be observed with a few Trotter steps. We now turn to a discussion of the most relevant errors included in this simulation, highlighting the advantage of our proposal in comparison to a traditional qubit-based approach.

Experimental gate errors can be drastically reduced by using qudits instead of qubits, due a substantial reduction of the required entangling operations. We illustrate this fact in Figs. 2(c) and 2(d) for the elementary group-multiplication gate $\Theta_{\ell|\ell'}$, where we compare the state fidelity of a maximally entangled state, $|\psi_1\rangle = 1/\sqrt{d}\sum_g |g\rangle|g\rangle$, prepared from a product state $|\psi_0\rangle = 1/\sqrt{d}\sum_g |0\rangle|g\rangle$ with $|\psi_1\rangle = \Theta|\psi_0\rangle$. Choosing $\Omega T = 3 \times 10^2$, $V/\Omega = 5$, and

$\gamma_e/\Omega = \gamma_r/\Omega = 10^{-6}$, we find a state fidelity of 99.6% for the qudit approach [87], in comparison to 21.4% for a qubit-based decomposition [see Fig. 1(c) and [82] for details of the employed decompositions [89]], demonstrating a clear advantage of the qudits. Similarly, the physical time required to implement one Trotter step [Fig. 1(a)] is drastically reduced by the qudit approach. We estimate a Trotter step time of $\sim 10^3 T$, taking into account a moving velocity below certain threshold to avoid decoherence [53], and using the structure of the group permutation matrices to reduce the number of pulses required to implement $\Theta_{\ell|\ell'}$ to $2(2d-1)(d-1)$ [82]. For $\Omega = 2\pi \times 100$ MHz, this leads to a Trotter step time of ~ 1 ms in contrast to ~ 100 ms [82] for a qubit-based approach. In summary, qudits enable the simulation of several Trotter steps within the experimental coherence times of NISQ devices with reasonable fidelity, while an analogous qubit simulation is experimentally unfeasible in the foreseeable future.

In the long run, a faithful quantum simulation of gauge theories in the field theory limit will also require a treatment of systematic errors, such as a finite Trotter step, finite lattice spacing, finite volume and finite subgroup. For brevity, we focus on the finite Trotter step here and briefly comment on other discretization errors in the conclusion. At fixed simulation time t, the Trotter error can be systematically reduced by decreasing δt at the cost of accumulating experimental gate errors. We quantify this competition for the simulated quantum computation in Fig. 3(a), where we plot the infidelity $1-\mathcal{F}$ of the evolution as a function of the Trotter step δt for $t\lambda_B = 1$. Comparing exact simulations of a second order Trotter decomposition to a simulation including the faulty group-multiplication gate described above, we quantify the overall accuracy by the overlap of the simulated state (Trotter evolved) $|\psi_{\mathrm{sim}}\rangle$ with the exact result $|\psi_{\mathrm{exact}}\rangle$, i.e., $\mathcal{F} = |\langle\psi_{\mathrm{sim}}|\psi_{\mathrm{exact}}\rangle|^2$. While the power-law behavior observed for the exact circuit clearly shows the proper convergence of the Trotter expansion, the realistic simulation is limited by a finite decay rate per Trotter step [Fig. 3(b)]. As a consequence, there is an optimal Trotter step as indicated in Fig. 3(a), leading to the best overall performance while minimizing the execution time of the simulation.

Conclusions and outlook.—A prerequisite to quantum simulation of non-Abelian LGTs with NISQ devices is hardware efficient encoding and processing with tailored, and scalable quantum hardware. The present work proposes a qudit-based architecture based on atoms stored in tweezer arrays, where single-qudit and entangling gates arising natively in qudit Rydberg-platforms are precisely those required for the simulation of LGTs. We show how our protocol leads to a significantly higher fidelity than a traditional qubit-based approach, which puts non-Abelian LGTs within reach of near-term quantum devices. Moreover, the present work can be extended to include dynamical matter [90], a necessary step towards addressing open questions in and beyond the standard model with quantum simulators. Finally, the qudit architecture outlined in this work provides a natural setting for systems with higher spin, for instance, for condensed-matter models or quantum chemistry applications [91].

We thank L. Pastori, H. Pichler, T. Olsacher, R. van Bijnen, and E. Zohar for valuable discussions. This work was supported by the U.S. Air Force Office of Scientific Research (AFOSR) via IOE Grant No. FA9550-19-1-7044 LASCEM, the European Union's Horizon 2020 research and innovation program under Grant Agreement No. 817482 (PASQuanS), and by the Simons Collaboration on Ultra-Quantum Matter, which is a grant from the Simons Foundation (651440, P. Z.). J. C. and B. K. are grateful for the support of the Austrian Science Fund (FWF): stand alone project P32273-N27 and the SFB BeyondC F 7107-N38.

*These authors contributed equally.
†daniel.gonzalez-cuadra@uibk.ac.at
‡torsten.zache@uibk.ac.at

[1] S. Weinberg, *The Quantum Theory of Fields* (Cambridge University Press, Cambridge, England, 1995), Vol. 2.
[2] I. Montvay and G. Münster, *Quantum Fields on a Lattice* (Cambridge University Press, Cambridge, England, 1997).
[3] S. Aoki *et al.*, Flag review 2019, Eur. Phys. J. C **80**, 113 (2020).
[4] M. Troyer and U.-J. Wiese, Computational Complexity and Fundamental Limitations to Fermionic Quantum Monte Carlo Simulations, Phys. Rev. Lett. **94**, 170201 (2005).
[5] N. Brambilla *et al.*, QCD and strongly coupled gauge theories: Challenges and perspectives, Eur. Phys. J. C **74**, 2981 (2014).
[6] J. Berges, M. P. Heller, A. Mazeliauskas, and R. Venugopalan, QCD thermalization: Ab initio approaches and interdisciplinary connections, Rev. Mod. Phys. **93**, 035003 (2021).
[7] R. P. Feynman, Simulating physics with computers, Int. J. Theor. Phys. **21**, 467 (1981).
[8] U.-J. Wiese, Ultracold quantum gases and lattice systems: Quantum simulation of lattice gauge theories, Ann. Phys. (Berlin) **525**, 777 (2013).
[9] E. Zohar, J. I. Cirac, and B. Reznik, Quantum simulations of lattice gauge theories using ultracold atoms in optical lattices, Rep. Prog. Phys. **79**, 014401 (2015).
[10] M. Dalmonte and S. Montangero, Lattice gauge theory simulations in the quantum information era, Contemp. Phys. **57**, 388 (2016).
[11] M. C. Bañuls *et al.*, Simulating lattice gauge theories within quantum technologies, Eur. Phys. J. D **74**, 165 (2020).
[12] M. Aidelsburger *et al.*, Cold atoms meet lattice gauge theory, Phil. Trans. R. Soc. A **380**, 20210064 (2022).
[13] E. Zohar, Quantum simulation of lattice gauge theories in more than one space dimension—requirements, challenges and methods, Phil. Trans. R. Soc. A **380**, 20210069 (2022).

[14] E. A. Martinez, C. A. Muschik, P. Schindler, D. Nigg, A. Erhard, M. Heyl, P. Hauke, M. Dalmonte, T. Monz, P. Zoller, and R. Blatt, Real-time dynamics of lattice gauge theories with a few-qubit quantum computer, Nature (London) **534**, 516 (2016).

[15] C. Schweizer, F. Grusdt, M. Berngruber, L. Barbiero, E. Demler, N. Goldman, I. Bloch, and M. Aidelsburger, Floquet approach to $\mathbb{Z}_2$ lattice gauge theories with ultracold atoms in optical lattices, Nat. Phys. **15**, 1168 (2019).

[16] C. Kokail, C. Maier, R. van Bijnen, T. Brydges, M. K. Joshi, P. Jurcevic, C. A. Muschik, P. Silvi, R. Blatt, C. F. Roos, and P. Zoller, Self-verifying variational quantum simulation of lattice models, Nature (London) **569**, 355 (2019).

[17] A. Mil, T. V. Zache, A. Hegde, A. Xia, R. P. Bhatt, M. K. Oberthaler, P. Hauke, J. Berges, and F. Jendrzejewski, A scalable realization of local U(1) gauge invariance in cold atomic mixtures, Science **367**, 1128 (2020).

[18] B. Yang, H. Sun, R. Ott, H.-Y. Wang, T. V. Zache, J. C. Halimeh, Z.-S. Yuan, P. Hauke, and J.-W. Pan, Observation of gauge invariance in a 71-site Bose–Hubbard quantum simulator, Nature (London) **587**, 392 (2020).

[19] Z.-Y. Zhou, G.-X. Su, J. C. Halimeh, R. Ott, H. Sun, P. Hauke, B. Yang, Z.-S. Yuan, J. Berges, and J.-W. Pan, Thermalization dynamics of a gauge theory on a quantum simulator, Science **377**, 311 (2022).

[20] N. H. Nguyen, M. C. Tran, Y. Zhu, A. M. Green, C. Huerta Alderete, Z. Davoudi, and N. M. Linke, Digital quantum simulation of the Schwinger model and symmetry protection with trapped ions, arXiv:2112.14262.

[21] N. Klco, A. Roggero, and M. J. Savage, Standard model physics and the digital quantum revolution: Thoughts about the interface, Rep. Prog. Phys. **85**, 064301 (2022).

[22] C. Muschik, M. Heyl, E. Martinez, T. Monz, P. Schindler, B. Vogell, M. Dalmonte, P. Hauke, R. Blatt, and P. Zoller, U(1) wilson lattice gauge theories in digital quantum simulators, New J. Phys. **19**, 103020 (2017).

[23] D. Paulson, L. Dellantonio, J. F. Haase, A. Celi, A. Kan, A. Jena, C. Kokail, R. van Bijnen, K. Jansen, P. Zoller, and C. A. Muschik, Simulating 2d effects in lattice gauge theories on a quantum computer, PRX Quantum **2**, 030334 (2021).

[24] Z. Davoudi, N. M. Linke, and G. Pagano, Toward simulating quantum field theories with controlled phonon-ion dynamics: A hybrid analog-digital approach, Phys. Rev. Res. **3**, 043072 (2021).

[25] L. Tagliacozzo, A. Celi, P. Orland, M. W. Mitchell, and M. Lewenstein, Simulation of non-Abelian gauge theories with optical lattices, Nat. Commun. **4**, 2615 (2013).

[26] L. Tagliacozzo, A. Celi, A. Zamora, and M. Lewenstein, Optical Abelian lattice gauge theories, Ann. Phys. (Amsterdam) **330**, 160 (2013).

[27] E. Zohar, A. Farace, B. Reznik, and J. I. Cirac, Digital Quantum Simulation of F_2 Lattice Gauge Theories with Dynamical Fermionic Matter, Phys. Rev. Lett. **118**, 070501 (2017).

[28] E. Zohar, A. Farace, B. Reznik, and J. I. Cirac, Digital lattice gauge theories, Phys. Rev. A **95**, 023604 (2017).

[29] J. Bender, E. Zohar, A. Farace, and J. I. Cirac, Digital quantum simulation of lattice gauge theories in three spatial dimensions, New J. Phys. **20**, 093001 (2018).

[30] A. Mezzacapo, E. Rico, C. Sabín, I. L. Egusquiza, L. Lamata, and E. Solano, Non-Abelian SU(2) Lattice Gauge Theories in Superconducting Circuits, Phys. Rev. Lett. **115**, 240502 (2015).

[31] N. Klco, E. F. Dumitrescu, A. J. McCaskey, T. D. Morris, R. C. Pooser, M. Sanz, E. Solano, P. Lougovski, and M. J. Savage, Quantum-classical computation of Schwinger model dynamics using quantum computers, Phys. Rev. A **98**, 032331 (2018).

[32] Y. Y. Atas, J. Zhang, R. Lewis, A. Jahanpour, J. F. Haase, and C. A. Muschik, SU(2) hadrons on a quantum computer via a variational approach, Nat. Commun. **12**, 6499 (2021).

[33] T. Armon, S. Ashkenazi, G. García-Moreno, A. González-Tudela, and E. Zohar, Photon-Mediated Stroboscopic Quantum Simulation of a F_2 Lattice Gauge Theory, Phys. Rev. Lett. **127**, 250501 (2021).

[34] J. Preskill, Quantum computing in the NISQ era and beyond, Quantum **2**, 79 (2018).

[35] T. Byrnes and Y. Yamamoto, Simulating lattice gauge theories on a quantum computer, Phys. Rev. A **73**, 022328 (2006).

[36] H. Lamm, S. Lawrence, and Y. Yamauchi (NuQS Collaboration), General methods for digital quantum simulation of gauge theories, Phys. Rev. D **100**, 034518 (2019).

[37] A. Alexandru, P. F. Bedaque, S. Harmalkar, H. Lamm, S. Lawrence, and N. C. Warrington (NuQS Collaboration), Gluon field digitization for quantum computers, Phys. Rev. D **100**, 114501 (2019).

[38] Y. Ji, H. Lamm, and S. Zhu (NuQS Collaboration), Gluon field digitization via group space decimation for quantum computers, Phys. Rev. D **102**, 114513 (2020).

[39] S. V. Mathis, G. Mazzola, and I. Tavernelli, Toward scalable simulations of lattice gauge theories on quantum computers, Phys. Rev. D **102**, 094501 (2020).

[40] D. B. Kaplan and J. R. Stryker, Gauss's law, duality, and the hamiltonian formulation of U(1) lattice gauge theory, Phys. Rev. D **102**, 094515 (2020).

[41] R. C. Brower, D. Berenstein, and H. Kawai, Lattice gauge theory for a quantum computer, Proc. Sci., LATTICE2019 (**2020**) 112 [arXiv:2002.10028].

[42] A. F. Shaw, P. Lougovski, J. R. Stryker, and N. Wiebe, Quantum algorithms for simulating the lattice Schwinger model, Quantum **4**, 306 (2020).

[43] N. Klco, M. J. Savage, and J. R. Stryker, SU(2) non-Abelian gauge field theory in one dimension on digital quantum computers, Phys. Rev. D **101**, 074512 (2020).

[44] A. Ciavarella, N. Klco, and M. J. Savage, Trailhead for quantum simulation of SU(3) Yang-Mills lattice gauge theory in the local multiplet basis, Phys. Rev. D **103**, 094501 (2021).

[45] A. Alexandru, P. F. Bedaque, R. Brett, and H. Lamm, The spectrum of qubitized QCD: Glueballs in a $S(1080)$ gauge theory, Phys. Rev. D **105**, 114508 (2022).

[46] J. F. Haase, L. Dellantonio, A. Celi, D. Paulson, A. Kan, K. Jansen, and C. A. Muschik, A resource efficient approach for quantum and classical simulations of gauge theories in particle physics, Quantum **5**, 393 (2021).

[47] C. W. Bauer and D. M. Grabowska, Efficient representation for simulating U(1) gauge theories on digital quantum computers at all values of the coupling, arXiv:2111.08015.

[48] A. Kan and Y. Nam, Lattice quantum chromodynamics and electrodynamics on a universal quantum computer, arXiv:2107.12769.
[49] Z. Davoudi, I. Raychowdhury, and A. Shaw, Search for efficient formulations for hamiltonian simulation of non-Abelian lattice gauge theories, Phys. Rev. D **104**, 074505 (2021).
[50] A. M. Kaufman and K.-K. Ni, Quantum science with optical tweezer arrays of ultracold atoms and molecules, Nat. Phys. **17**, 1324 (2021).
[51] M. Saffman, Quantum computing with atomic qubits and Rydberg interactions: Progress and challenges, J. Phys. B **49**, 202001 (2016).
[52] L. Henriet, L. Beguin, A. Signoles, T. Lahaye, A. Browaeys, G.-O. Reymond, and C. Jurczak, Quantum computing with neutral atoms, Quantum **4**, 327 (2020).
[53] D. Bluvstein, H. Levine, G. Semeghini, T. T. Wang, S. Ebadi, M. Kalinowski, A. Keesling, N. Maskara, H. Pichler, M. Greiner, V. Vuletić, and M. D. Lukin, A quantum processor based on coherent transport of entangled atom arrays, Nature (London) **604**, 451 (2022).
[54] S. R. Cohen and J. D. Thompson, Quantum computing with circular rydberg atoms, PRX Quantum **2**, 030322 (2021).
[55] E. Guardado-Sanchez, B. M. Spar, P. Schauss, R. Belyansky, J. T. Young, P. Bienias, A. V. Gorshkov, T. Iadecola, and W. S. Bakr, Quench Dynamics of a Fermi Gas with Strong Nonlocal Interactions, Phys. Rev. X **11**, 021036 (2021).
[56] I. S. Madjarov, J. P. Covey, A. L. Shaw, J. Choi, A. Kale, A. Cooper, H. Pichler, V. Schkolnik, J. R. Williams, and M. Endres, High-fidelity entanglement and detection of alkaline-earth Rydberg atoms, Nat. Phys. **16**, 857 (2020).
[57] V. Kasper, D. González-Cuadra, A. Hegde, A. Xia, A. Dauphin, F. Huber, E. Tiemann, M. Lewenstein, F. Jendrzejewski, and P. Hauke, Universal quantum computation and quantum error correction with ultracold atomic mixtures, Quantum Sci. Technol. **7**, 015008 (2021).
[58] M. Ringbauer, M. Meth, L. Postler, R. Stricker, R. Blatt, P. Schindler, and T. Monz, A universal qudit quantum processor with trapped ions, Nat. Phys. **18**, 1053 (2022).
[59] Y. Chi *et al.*, A programmable qudit-based quantum processor, Nat. Commun. **13**, 1166 (2022).
[60] H. Levine, A. Keesling, G. Semeghini, A. Omran, T. T. Wang, S. Ebadi, H. Bernien, M. Greiner, V. Vuletić, H. Pichler, and M. D. Lukin, Parallel Implementation of High-Fidelity Multiqubit Gates with Neutral Atoms, Phys. Rev. Lett. **123**, 170503 (2019).
[61] S. Ebadi, T. T. Wang, H. Levine, A. Keesling, G. Semeghini, A. Omran, D. Bluvstein, R. Samajdar, H. Pichler, W. W. Ho, S. Choi, S. Sachdev, M. Greiner, V. Vuletić, and M. D. Lukin, Quantum phases of matter on a 256-atom programmable quantum simulator, Nature (London) **595**, 227 (2021).
[62] P. Scholl, M. Schuler, H. J. Williams, A. A. Eberharter, D. Barredo, K.-N. Schymik, V. Lienhard, L.-P. Henry, T. C. Lang, T. Lahaye, A. M. Läuchli, and A. Browaeys, Quantum simulation of 2D antiferromagnets with hundreds of Rydberg atoms, Nature (London) **595**, 233 (2021).
[63] A. W. Young, W. J. Eckner, N. Schine, A. M. Childs, and A. M. Kaufman, Tweezer-programmable 2D quantum walks in a Hubbard-regime lattice, Science **377**, 885 (2022).
[64] Y. Wang, Z. Hu, B. C. Sanders, and S. Kais, Qudits and high-dimensional quantum computing, Front. Phys. **8**, 589504 (2020).
[65] E. J. Gustafson, Prospects for simulating a qudit-based model of $(1+1)$D scalar QED, Phys. Rev. D **103**, 114505 (2021).
[66] E. Gustafson, Noise improvements in quantum simulations of sQED using qutrits, arXiv:2201.04546.
[67] M. Saffman, T. G. Walker, and K. Mølmer, Quantum information with Rydberg atoms, Rev. Mod. Phys. **82**, 2313 (2010).
[68] P. Zanardi and M. Rasetti, Holonomic quantum computation, Phys. Lett. A **264**, 94 (1999).
[69] E. Sjöqvist, D. M. Tong, L. M. Andersson, B. Hessmo, M. Johansson, and K. Singh, Non-adiabatic holonomic quantum computation, New J. Phys. **14**, 103035 (2012).
[70] G. F. Xu, J. Zhang, D. M. Tong, E. Sjöqvist, and L. C. Kwek, Nonadiabatic Holonomic Quantum Computation in Decoherence-Free Subspaces, Phys. Rev. Lett. **109**, 170501 (2012).
[71] G. Feng, G. Xu, and G. Long, Experimental Realization of Nonadiabatic Holonomic Quantum Computation, Phys. Rev. Lett. **110**, 190501 (2013).
[72] Y.-H. Kang, Y.-H. Chen, Z.-C. Shi, B.-H. Huang, J. Song, and Y. Xia, Nonadiabatic holonomic quantum computation using Rydberg blockade, Phys. Rev. A **97**, 042336 (2018).
[73] Note that the advantage of using qudits has also been recently demonstrated in the context QAOA [74].
[74] J. R. Weggemans, A. Urech, A. Rausch, R. Spreeuw, R. Boucherie, F. Schreck, K. Schoutens, J. Minář, and F. Speelman, Solving correlation clustering with QAOA and a Rydberg qudit system: A full-stack approach, Quantum **6**, 687 (2022).
[75] M. A. Levin and X.-G. Wen, String-net condensation: A physical mechanism for topological phases, Phys. Rev. B **71**, 045110 (2005).
[76] C. Xu and A. W. W. Ludwig, Topological Quantum Liquids with Quaternion Non-Abelian Statistics, Phys. Rev. Lett. **108**, 047202 (2012).
[77] A. Trautmann, M. J. Mark, P. Ilzhöfer, H. Edri, A. E. Arrach, J. G. Maloberti, C. H. Greene, F. Robicheaux, and F. Ferlaino, Spectroscopy of Rydberg states in erbium using electromagnetically induced transparency, Phys. Rev. Res. **3**, 033165 (2021).
[78] M. Saffman and K. Mølmer, Scaling the neutral-atom Rydberg gate quantum computer by collective encoding in holmium atoms, Phys. Rev. A **78**, 012336 (2008).
[79] J. Hostetter, J. D. Pritchard, J. E. Lawler, and M. Saffman, Measurement of holmium Rydberg series through magneto-optical trap depletion spectroscopy, Phys. Rev. A **91**, 012507 (2015).
[80] G. F. Xu, P. Z. Zhao, E. Sjöqvist, and D. M. Tong, Realizing nonadiabatic holonomic quantum computation beyond the three-level setting, Phys. Rev. A **103**, 052605 (2021).
[81] C.-K. Li, R. Roberts, and X. Yin, Decomposition of unitary matrices and quantum gates, Int. J. Quantum. Inform. **11**, 1350015 (2013).
[82] See Supplemental Material at http://link.aps.org/supplemental/10.1103/PhysRevLett.129.160501 for further details on the implementation of holonomic gates and the

digital quantum simulation of the Q_8 LGT, including a comparison with a qubit-based protocol.
[83] J. Carrasco *et al.* (to be published).
[84] J. Kogut and L. Susskind, Hamiltonian formulation of Wilson's lattice gauge theories, Phys. Rev. D **11**, 395 (1975).
[85] H. F. Trotter, On the product of semi-groups of operators, Proc. Am. Math. Soc. **10**, 545 (1959).
[86] N. Hatano and M. Suzuki, Finding exponential product formulas of higher orders, in *Quantum Annealing and Other Optimization Methods*, edited by A. Das and B. K. Chakrabarti (Springer Berlin Heidelberg, Berlin, Heidelberg, 2005), pp. 37–68.
[87] We note that the fidelity of the group-multiplication gate could be further improved through optimal-control methods [88], where other experimental imperfections such as phase errors due to Stark shifts could be taken into account.
[88] S. Jandura and G. Pupillo, Time-optimal two- and three-qubit gates for Rydberg atoms, Quantum **6**, 712 (2022).
[89] Note that, even if the qubit decomposition found is not necessarily the optimal one, improved decompositions are not expected to qualitatively change these results.
[90] D. González-Cuadra *et al.* (to be published).
[91] S. McArdle, S. Endo, A. Aspuru-Guzik, S. C. Benjamin, and X. Yuan, Quantum computational chemistry, Rev. Mod. Phys. **92**, 015003 (2020).